van der Waals epitaxial growth and characterization of $MoSe_2$ thin films on SnS_2

F. S. Ohuchi and B. A. Parkinson
Central Research and Development Department, E. I. DuPont de Nemours and Company, Wilmington, Delaware 19880

K. Ueno and A. Koma
Department of Chemistry, The University of Tokyo, Bunkyo-ku, Tokyo 113, Japan

(Received 9 March 1990; accepted for publication 16 May 1990)

A variation on molecular beam epitaxy (MBE), called van der Waals epitaxy, is described where a material with primarily two-dimensional (2D) bonding is grown on a substrate which also has a 2D structure. Lattice matching difficulties, which limit the choice of materials in MBE of 3D systems, are circumvented since the interlayer bonding is from weak van der Waals interactions. The title system shows a lattice mismatch of 10% yet high quality epitaxial films can be grown. The films were characterized *in situ* with reflection high energy electron diffraction, Auger electron spectroscopy, and low energy electron loss spectroscopy. Additional characterization after exposure to ambient by x-ray photoelectron spectroscopy, low energy electron diffraction, transmission electron microscopy confirmed the highly ordered nature of the films. Scanning tunneling microscopy provided real space images of the morphology of the epitaxial layer and showed unusual structures attributed to lattice mismatch.

I. INTRODUCTION

The potential for new materials with tailored bulk, surface, and interface properties has motivated many recent investigations concerned with fabricating semiconductor based heterostructures. Molecular beam epitaxy (MBE) has proven to be an indispensable tool in this field, where atomically smooth and abrupt interfaces can be fabricated. While nearly perfect MBE growth has been demonstrated in many cases, the choice of the heteroepitaxial systems is limited by the factors dictated by the materials themselves, i.e., surface dangling bonds, surface states, surface symmetry, ability to clean the surface, and lattice mismatch between the two materials. In addition, the difference in the thermal expansions coefficients between epilayer and substrate result in appreciable thermal stresses at the interface.

van der Waals epitaxy (VDWE), a method recently developed by Koma,[1,2] opens up a new route to heteroepitaxy without most of the constraints mentioned above. VDWE is a growth of several of several 2D metal chalcogenide materials, one upon the other, where the layers are bound together by weak van der Waals forces. Many metal dichalcogenides are two-dimensional materials with structures characterized by chalcogen–metal–chalcogen layers (herein, defined as "one unit layer") held together by van der Waals forces. Cleavage results in exposing a low free energy van der Waals surface composed of an inert sheet of hexagonal-closed-packed chalcogen atoms. Changing either the metal or chalcogen atom may alter the electronic character, metal atom coordination, or intraplanar crystal structure of the material while preserving the layered structure. Because of the 2D nature of metal dichalcogenide surfaces, there are no dangling bonds associated with the surface. In addition, lattice mismatch is not problematic due to the lack of covalent bonding across the van der Waals gaps of the two materials.

In Fig. 1, the conceptional difference between a conventional heterointerface and an interface fabricated via the van der Waals epitaxial growth is depicted. In VDWE we expect formation of an atomically abrupt interface with minimum

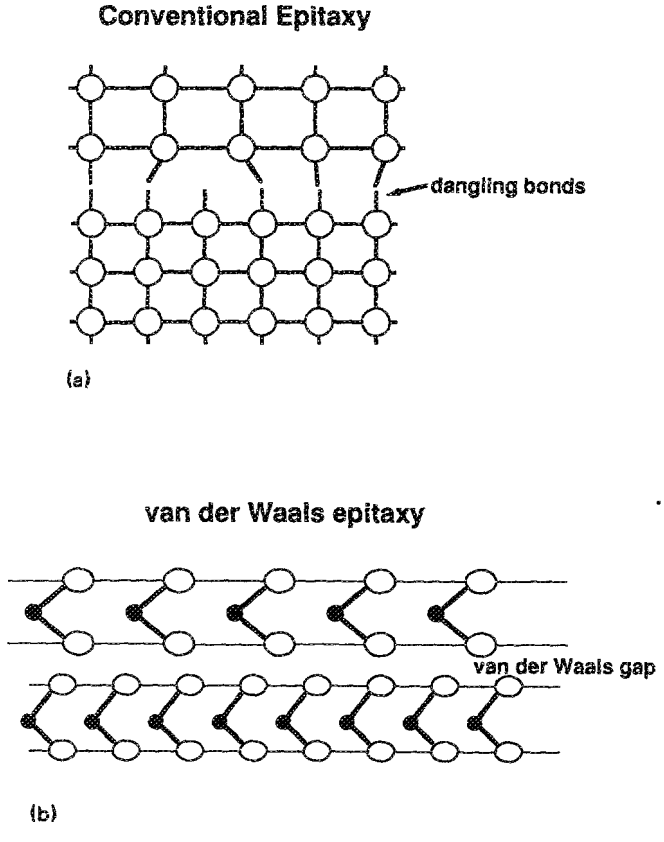

FIG. 1. Heterointerfaces fabricated by (a) conventional molecular beam epitaxy and (b) van der Waals epitaxy.

 0021-8979/90/172168-08$03.00

defect density regardless of large lattice mismatches. The potential flexibility for construction of complex layered structures containing different materials selected for their specific electronic properties, rather than their lattice matches, makes this an exciting new area for investigation. Recent reports of the synthesis of bulk crystals of "misfit layered structure" materials, consisting of alternate layers of SnS and NbS_2, provide additional support of the possibility of VDWE.[3]

We report a thorough investigation of the fabrication and characterization of heterostructures of $MoSe_2$ thin films epitaxially grown on $SnS_2(0001)$. In the past, epilayers of $MoSe_2$ and $NbSe_2$ on MoS_2 have been prepared.[2,4] Also the preparation of heterojunctions of *n*-$MoSe_2$ on *p*-WSe_2[5] and *p–n* homojunctions of WSe_2[6] have been reported, however vapor transport was used rather than the much more flexible MBE technique. The substrate used in the present investigation differs from MoS_2 both electronically and structurally.[7] SnS_2 is more ionic, whereas MoS_2 is very covalent. The Sn is surrounded by six S atoms in an octahedral coordination, whereas the Mo in MoS_2 has a trigonal prismatic coordination. The band gap of SnS_2 is 2.2 eV, whereas the band gap of MoS_2 is 1.1 eV. The contrasts of these materials are also seen in their electronic structures, where chalcogen *p* states are the top of the valence band for SnS_2 whereas for MoS_2 the top of the valence band is composed of Mo-d_{z^2} states. While the identity of the substrate strongly influences the growth process in conventional epitaxy, it will be shown that for $MoSe_2/SnS_2$ a high quality atomically abrupt epitaxial thin film is obtained depsite a 10% lattice mismatch.

II. EXPERIMENT

The MBE system used in the present investigation was a built in house and consists of a three chambered, diffusion pumped, liquid nitrogen shrouded, apparatus, as shown in Fig. 2. The three chambers are a load-lock chamber for fast introduction of the substrate materials into vacuum, an analytical chamber for Auger electron spectroscopy (AES), and low energy electron energy loss spectroscopy (LEELS), and an epitaxy chamber equipped with MBE sources and reflection high energy electron diffraction (RHEED). Selenium was evaporated from a Knudsen cell normally operated at around 105 °C, and an electrostatically focused electron beam source was used for Mo evaporation.

Single crystals of *n*-SnS_2 (chlorine doped) prepared by a Bridgman technique were used as the substrate. Clean (0001) van der Waals surfaces were produced by cleaving the crystal in air via a sticky tape just prior to introduction into vacuum. Previously this technique has been shown to produce clean oxide free surfaces with large areas of atomic flatness.[8]

Growth of $MoSe_2$ was carried out at a substrate temperature of 400 °C in a Se rich atmosphere. The deposition rate was constantly monitored by a water cooled quartz oscillator and RHEED was used for a real-time monitoring of the growth process (typical operating voltage of 20 keV). The RHEED patterns were recorded with a 35 mm reflex camera using 400 ASA photographic film. Occasionally the

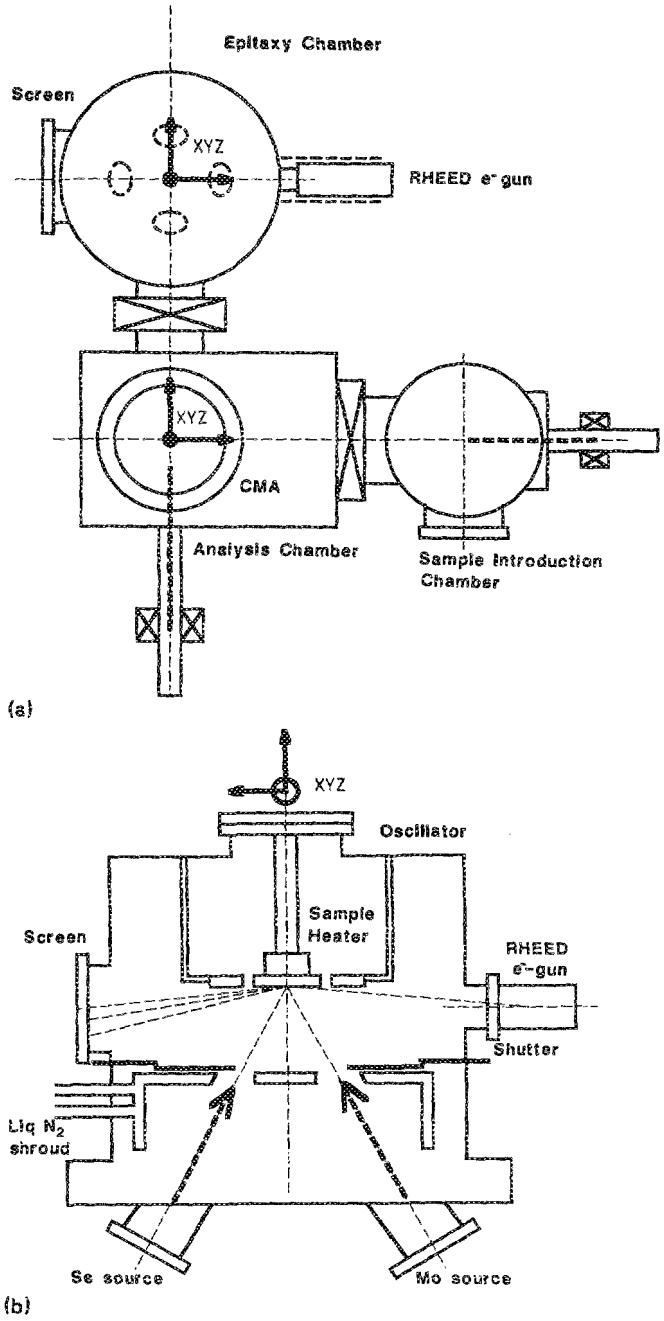

FIG. 2. Schematic illustrations of the main blocks of MBE system showing in (a) the chamber arrangement and (b) the cutaway part of the epitaxy chamber.

growth was interupted and the sample was transferred back to the analysis chamber for *in situ* characterization by AES and LEELS. A double pass cylindrical mirror analyzer (CMA, PHI 15-255G) was used for both analyses. In particular for LEELS, a retarding mode with pulse counting was employed to assure a constant energy resolution of 0.4 eV in the energy range between 30 and 2000 eV.

After growth of the desired thickness of $MoSe_2$ the specimens were taken out from the vacuum chamber and cut into two parts, one stored in a vacuum desiccator (100 mTorr) and the other in the laboratory atmosphere. These specimens were then characterized by x-ray photoelectron

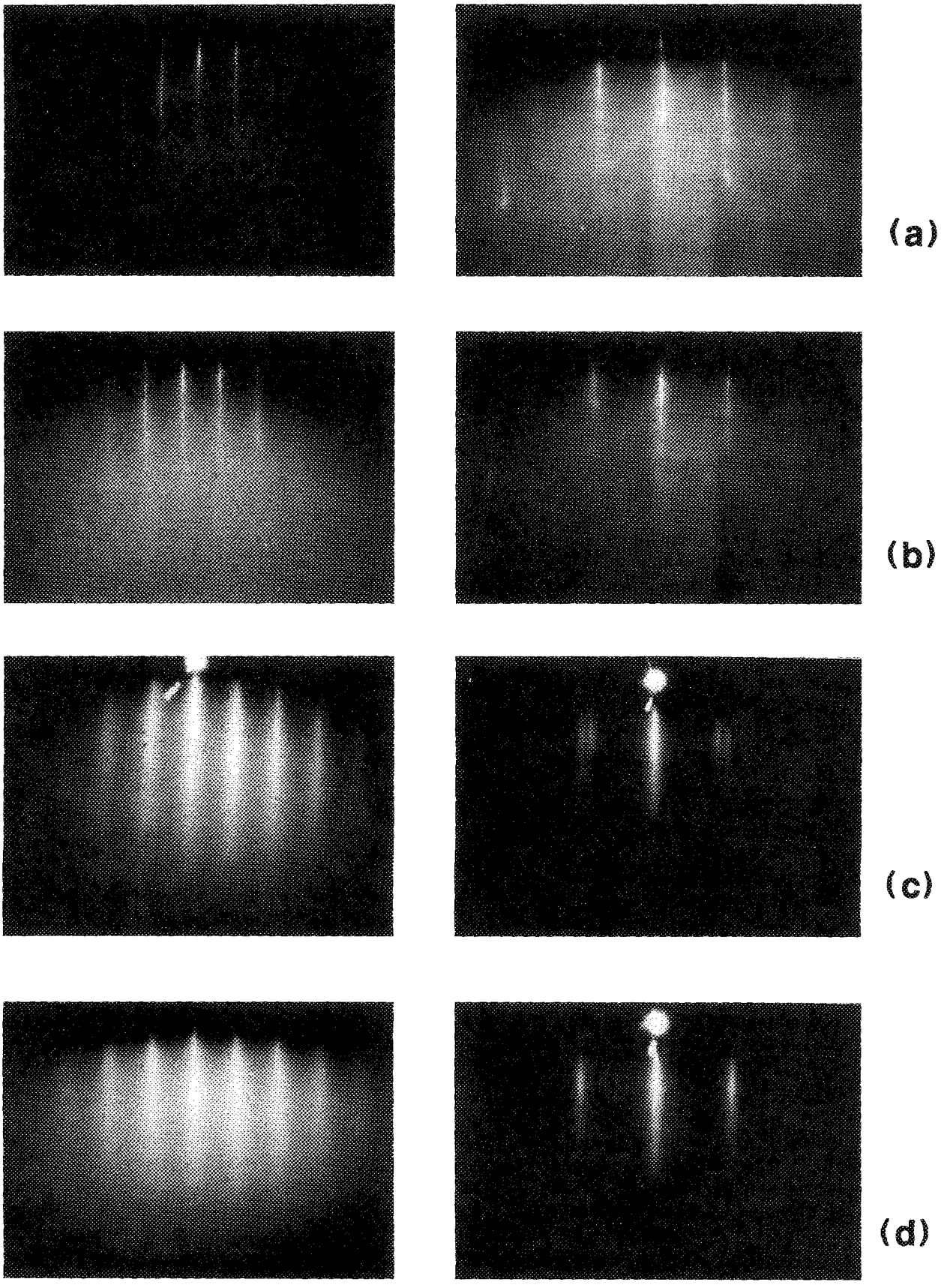

FIG. 3. RHEED patterns observed from $[11\bar{2}0]$ and $[10\bar{1}0]$ azimuthal angles. (a) (0001)SnS_2, (b) Se on (0001)SnS_2 at 400 °C, (c) $MoSe_2$ on (0001)SnS_2 with fractional coverage, (d) $MoSe_2$ layer after complete growth on SnS_2(0001).

spectroscopy (XPS), low energy electron diffraction (LEED), scanning tunneling microscopy (STM), and transmission electron microscopy (TEM) with selected area electron diffraction (SAD). All these investigations were performed within 75 days after fabrication. For XPS analysis, a monochoromatized x-ray source (Al-$K\alpha$) was used to excite the photoelectrons, and their energies were analyzed with a 180° hemispherical analyzer equipped with position sensitive detectors. The resolution achieved for Au($4f_{7/2}$) was about 0.7 eV. LEED was performed using conventional 4-grid optics. STM was performed in air using a Nanoscope II (Digigal Instruments) operating in the constant current mode with electrochemically etched platinum or tungsten tips. Tunneling currents and voltages are indicated on the individual images. Subsequent to XPS, LEED, and STM analyses the samples were analyzed with electron microscopy. A fine needle was used to scrape off a small portion of the specimen surface some of which was collected over carbon coated 200 mesh Cu grid. A JEOL 2000-FX transmission electron microscope with an operating voltage of 200 keV was usef for imaging and selected area diffraction.

III. RESULTS

A. Growth

Shown in Fig. 3 are a series of RHEED pattern transitions acquired during the epitaxial growth of $MoSe_2$. First, the patterns from a clean (0001)SnS_2, observed from [$11\bar{2}0$] and [$10\bar{1}0$] azimuthal angles (Fig. 3(a)], indicate that there is no reconstruction of the surface. The elongated streaks and well-developed Kikuchi patterns suggest good crystalline quality and a smooth surface. The RHEED patterns did not deteriorate over prolonged time. The surface was then exposed to a Se flux at 400 °C prior to initiation of Mo deposition. No changes in the streak intervals were identified, indicating that the Se species do not adsorb or react with the surface [Fig. 3(b)]. When the Mo flux was initiated, the substrate patterns immediately faded out for a few minutes and then reappeared as the deposition proceeded. A typical growth rate was 0.1 nm/min at the substrate temperature of 400 °C. After several more minutes of deposition, additional streaks along with the substrate pattern for both azimuthal angles appeared [Fig. 3(c)]. Coexistence of both substrate and deposite RHEED streaks is an indication of deposition of a fraction of one unit layer. The lattice constant for the deposit calculated from the streak intervals was 3.29 ± 0.05 Å, close to the published value of 3.288 Å for 2H-$MoSe_2$.[9] In addition, these streaks are aligned along the same azimuthal directions as the substrate, indicating that the overlayer is rotationally commensurate with respect to the substrate. Further growth of the $MoSe_2$ layer resulted in the substrate patterns completely fading out leaving only the epilayer streaks indicating formation of a well oriented crystalline $MoSe_2$ thin film [Fig. 3(d)].

B. *In situ* characterization by AES and LEELS

The chemical composition of the film was studied by *in situ* AES. Figure 4 shows AES spectra obtained from: (a) SnS_2 (single crystal), (b) $MoSe_2$ layer on SnS_2 with fractional coverage, (c) $MoSe_2$ after complete growth, and (d) cleaved $MoSe_2$ (single crystal). *In situ* heating of the substrate to 3000 °C in the analysis chamber was used to drive off surface contamination, but as indicated in Fig. 4(a), a small amount of carbon remained on the surface. This level of surface contamination apparently did not affect the epitaxial growth. The chemical composition of the epilayer after both fractional and multilayer growth was calculated by comparing the Auger peak heights for Se(MNN) at 43 eV and MO(MNN) at 185 eV with those measured from the single crystalline $MoSe_2$. The estimated composition was $MoSe_{2.5}$, substantially rich in Se. The excess Se in the film may be due to Se adsorption during specimen transfer from the growth to analytical chambers while the epitaxial chamber still contained a Se rich atmosphere and the sample had cooled from its deposition temperature. Nonetheless *in situ* AES analyses identifies the epilayer as crystalline $MoSe_2$ even at fractional monolayer coverages.

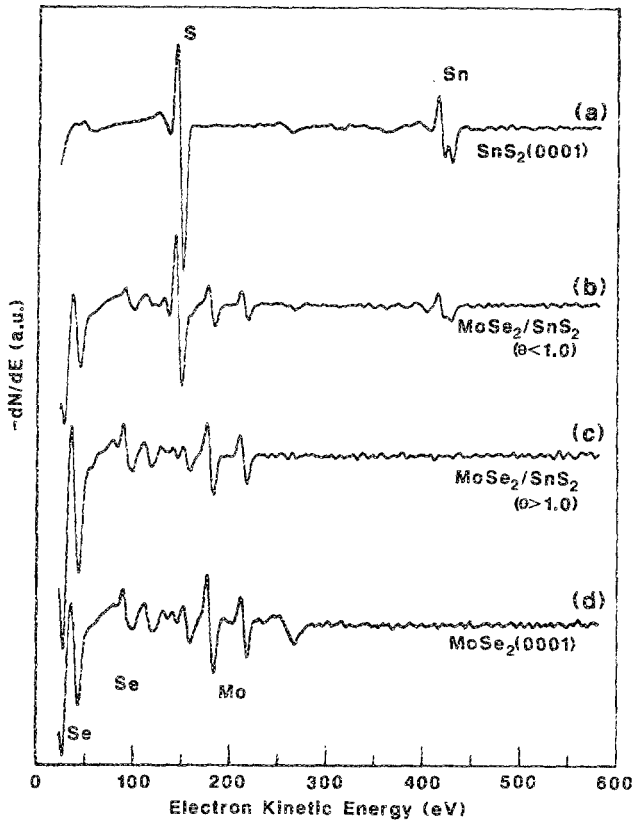

FIG. 4. AES spectra obtained from: (a) SnS_2 (single crystal), (b) $MoSe_2$ layer on SnS_2 with fractional coverage, (c) $MoSe_2$ after complete growth, and (d) cleaved $MoSe_2$ (single crystal).

Nondestructive depth profiling of the $MoSe_2/SnS_2$ heterostructure was carried out with LEELS, where the probing depth was varied from 0.4 to 1.0 nm by changing the incident electron energy from 200 to 1500 eV, respectively.[10] Shown in Fig. 5 are a series of LEELs spectra [in a second differentiated form, $-d^2N(E)/dE^2$] obtained at different probe energies after one unit layer of $MoSe_2$ film growth over the SnS_2(0001) substrate. Spectra obtained from single crys-

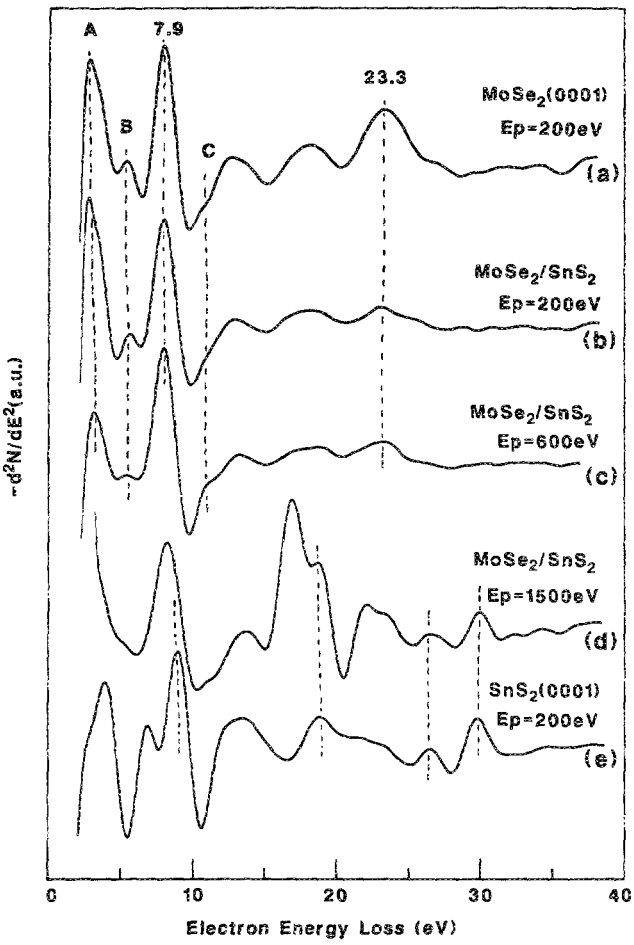

FIG. 5. LEELS spectra obtained from: (a) (0001) $MoSe_2$ single crystal, (b) $MoSe_2$ on SnS_2 at $Ep = 200$ eV, (c) at 600 eV, (d) at 1500 eV, and (e) (0001) SnS_2 single crystal.

tals of $MoSe_2$ and SnS_2 are also shown for comparison. Single crystal $MoSe_2$ [Fig. 5(a)] shows two prominent loss peaks at 7.9 and 23.3 eV [Although not shown here, these peaks are much more pronounced in $N(E)$.] These two peaks come from the excitations of partial plasmons and of bulk plasmons, following Liang and Cundy.[10] Loss peaks labeled by A, B, and C may be assigned to be the transitions from the p states of Se atoms to empty states above the Fermi level. The energy loss spectra from the $MoSe_2/SnS_2$ heterostructure were collected with incident energies of 200, 600, and 1500 eV and are shown in Figs. 5(b), 5(c), and 5(d), respectively. It is found that up to a probe energy of 600 eV, the spectra obtained from $MoSe_2/SnS_2$ heterostructure show nearly identical peak energies and relative intensities to spectra from single crystal $MoSe_2$. With higher probing energies, however, the spectrum changed rather drastically. The spectrum consists of all the peaks observed with lower primary electron energies and additional peaks at 18.8, 22.0, 26.4, and 29.8 eV. The partial plasmon peak at 8 eV was considerably broadened, suggesting peak overlap. Comparing this spectrum with one obtained from the single crystal SnS_2 [Fig. 5(e)], these additional peaks match those energies quite well. The peak at 29.8 eV corresponds to the Sn($4d$) core transition from the SnS_2.

The LEELS results suggest that the electronic structure of the MBE grown $MoSe_2$ films, even for one molecular layer, is close to that of crystalline $MoSe_2$. In addition, the absence of substrate signal at the LEELS probing energies below 600 eV, but identified at 1500 eV indicate that the $MoSe_2/SnS_2$ heterointerface must be flat and atomically sharp.

C. XPS/LEED

XPS was performed on samples after 75 days of storage in two different environments (desiccator vs laboratory). The sample stored in the vacuum desiccator showed very little carbon contamination or oxidation. The sample was then *in situ* heated to 300 °C to further remove surface contamination. Figure 6(a) shows the core level spectra for Se($3d$) and Mo($3d$). Based on the elemental sensitivity factors for Se and Mo, determined from the single crystal $MoSe_2$ specimen [Fig. 6 (c)], the calculated chemical composition of the film was $MoSe_{2.10\pm0.02}$, still slightly rich in Se. While the Se($3d$) spin–orbit splitting was well defined in the single crystal $MoSe_2$, a slight broadening was observed for the film. Broadening may arise from defects, crystalline disorder, lattice inclusion, lattice strain, etc., all of which should not be significant in this case. The binding energies of the Se($3d_{5/2}$) and Mo($3d_{5/2}$) core levels in the films are 54.67 and 229.06 eV, respectively, identical to the values observed with single crystalline $MoSe_2$, indicating that the band offset is negligible in the present system.

The specimen epxosed to the laboratory atmosphere for the extended time period showed surface oxidation as evidenced by development of additional peaks in both Se($3d$)

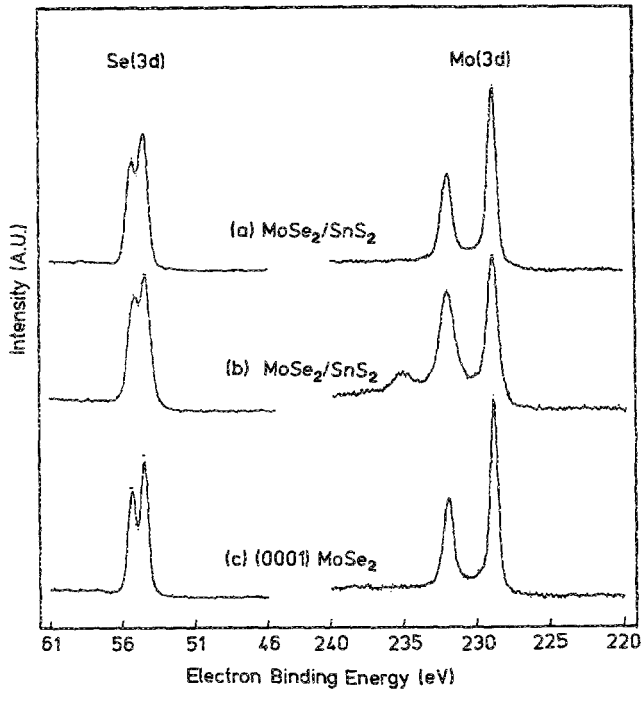

FIG. 6. XPS spectra obtained from $MoSe_2$ epilayers stored in two different environment: (a) desiccator and (b) laboratory atmosphere. Spectra (c) from (0001) $MoSe_2$ single crystal.

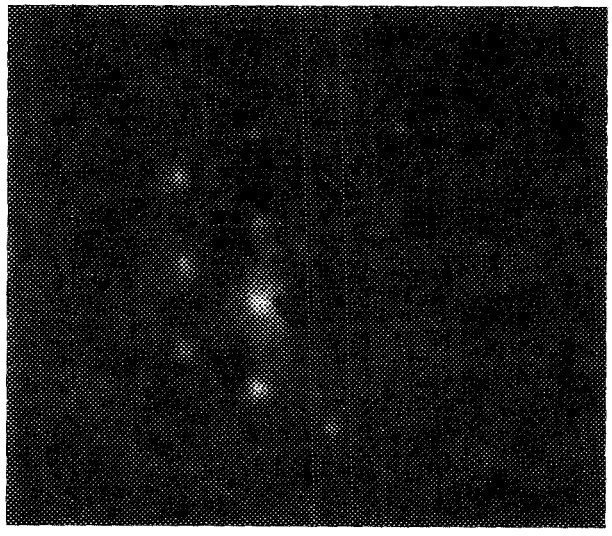

(a)

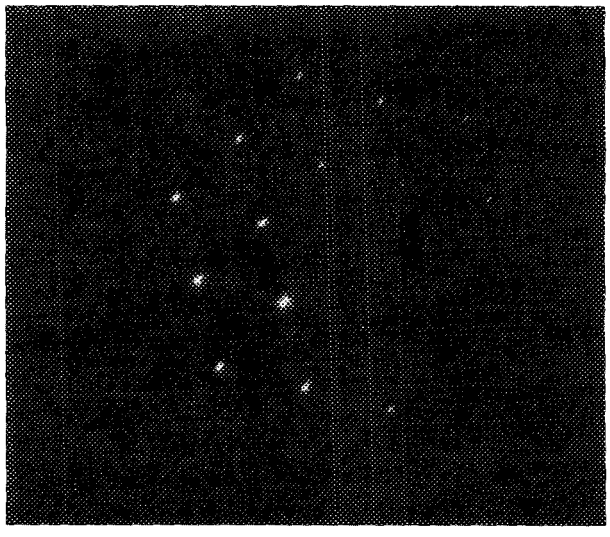

(b)

FIG. 7. LEED patterns from: (a) $MoSe_2$ epilayer and (b) (0001)$MoSe_2$ single crystal.

and Mo($3d$) regions [Fig. 6(b)] along with the O($1s$) peak. The spectra for the Se($3d$) and Mo($3d$) and Mo($3d$) peaks of this material were separated by a nonlinear least-squares technique which constrains the fit in accordance with the spin splittings and area ratios for both peaks. Removing these components, the remaining peaks result in the stoichiometry $MoSe_{2.11}$, nearly identical to the clean specimen. This indicates that only the top few molecular layers of $MoSe_2$ epitaxial layer was partially oxidized, below which the remaining $MoSe_2$ was unchanged. As will be discussed later, the top few $MoSe_2$ layers are not completed in the MBE process, therefore the oxidation of reactive dangling bonds from the edge of $MoSe_2$ islands accounts for the observed oxygen.

LEED was performed on a "vacuum stored" specimen after *in situ* heating to 300 °C to drive off possible contamination. The 144 eV LEED pattern observed from the specimen is shown in Fig. 7 along with the pattern from a cleaved $MoSe_2$ single crystal. Well defined hexagonal patterns are observed with identical spot to spot separations to those of single crystal $MoSe_2$. The spots from the epitaxial film were slightly diffuse which could result from either small domains or grain boundary effects, however, another cause will be discussed later in the STM section. The slight nonstoichiometry of the epitaxial film may also affect to the quality of diffraction.

D. TEM and SAD

TEM was utilized to further assess the microstructure of the $MoSe_2$ epitaxial films. Plane view specimens from single crystals of SnS_2 and $MoSe_2$, as well as $MoSe_2$ epitaxial thin film on SnS_2, were prepared as described previously. SAD patterns from both single crystals were obtained for internal calibrations. Figure 8 shows a SAD pattern from the $MoSe_2/SnS_2$ heterostructure. It is apparent that the observed SAD consists of a mixture of two rotationally aligned hexagonal patterns. Comparing with SAD patterns obtained from both single crystals, inner hexagonal patterns with sharper diffraction spots correspond to those from the SnS_2 substrate, while outer hexagonal patterns with slightly diffused spots are from $MoSe_2$ overlayers. The spots are mainly diffused in radial directions, and only a slight azimuthal rotation is noticed. In addition to the diffuseness of the spots, the fact that the two diffraction patterns are rotationally aligned

$MoSe_2/SnS_2$

FIG. 8. SAD pattern from the $MoSe_2/SnS_2$ heterostructure.

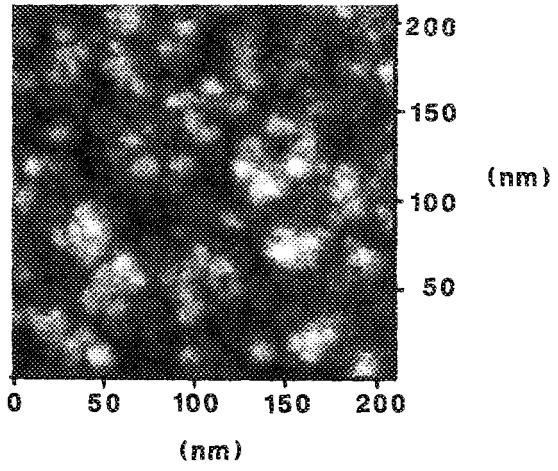

FIG. 9. STM image of a $MoSe_2$ epilayer with a 200 nm scan range taken at a constant current of 0.28 nA and a voltage of − 750 mV.

is strong evidence that the $MoSe_2$ overlayer has epitaxially grown onto SnS_2 with their hexagonal edges aligned. However, the alignment of the edges from each crystal may not be exact, which in turn represents slight ($< 1°$) azimuthal rotations in the pattern.

E. Scanning tunneling microscopy

Scanning tunneling microscopy, being a real space technique, nicely compliments the diffraction techniques for investigation of the morphology of the films. While there is a direct relationship between the real and reciprocal space images of structures, the diffraction techniques lose information about the morphology of the surface when the patterns are projected back into real space. In Fig. 9, a constant current STM image from the $MoSe_2$ film with a 200 nm scan range is shown, in which 40–50 nm domains can be observed. Many domain boundaries can be identified which intersect at angles within experimental error of 120° as would be expected for the intersection of hexagonal domains (single crystals of $MoSe_2$ nearly always form as hexagonal platelets). Analysis of the depth information of a 165 nm scan (Fig. 10) shows steps which within experimental error correlate with an integer number of c axis unit cell dimensions for $MoSe_2$ indicating that there are several incomplete layers sitting on top of many complete layers since the total epilayer thickness is several hundred angstroms. In several areas crevices can be seen which penetrate deeply but due to the finite size of the tip it cannot be determined whether they penetrate all the way to the substrate, however they are eventually filled with atoms to form complete layers.

A close look at the STM image in Fig. 10 reveals reproducible modulation at about ten times the size of atoms. Figure 11 shows an even higher magnification STM image 19 nm on a side. Triangular domains arranged to form "wagon wheel" structures are clearly visible. Although our first thought about VDWE was that lattice matching would not be a factor further thought reveals there are still more and less stable sites for van der Waals interactions between the two lattices. A lattice mismatch of 10% predicts that the lattices will go in and out of phase with about 33 Å between stable trigonal sites for epilayer atoms. The STM is extreme-

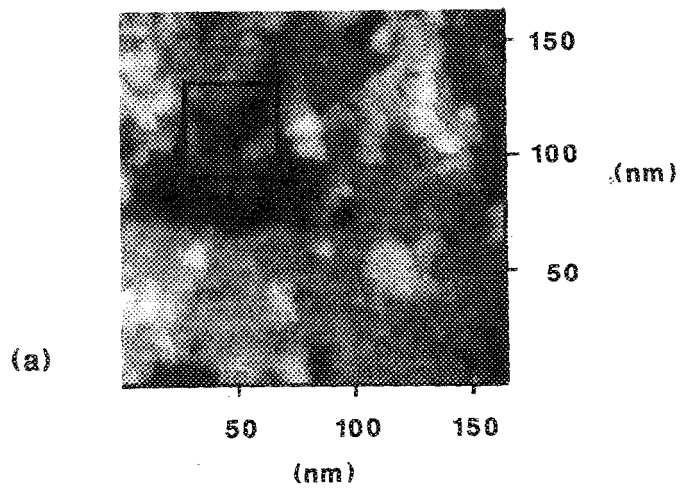

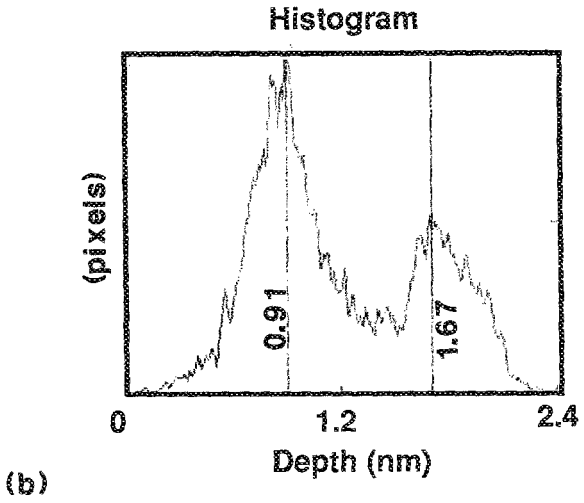

FIG. 10. A. STM image of a $MoSe_2$ epilayer with a 165 nm scan range with a tunneling current of 1.9 nA and a voltage of − 350 mV. B. Histogram of pixel depth within the square region.

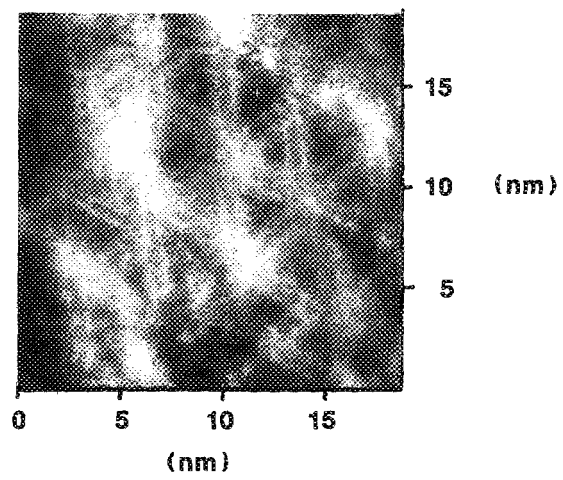

FIG. 11. Higher magnification STM image of $MoSe_2$ epilayer with a 19 nm scan range. The tunneling current was 0.33 nA and the voltage was − 574 mV.

ly sensitive to distance changes in the z direction (out of the plane) and so is able to discern these subtle structures. The triangular structures seen in Fig. 11 are about 30 to 50 Å across. A more detailed account of this lattice mismatch phenomena between van der Waals surfaces will be given elsewhere.[11]

IV. DISCUSSION

We have utilized a battery of techniques to elucidate the epitaxial relationship between two materials. All the data from various techniques were consistent and provided insight into the mechanism of VDWE. In particular, *in situ* RHEED and TEM-SAD provided direct evidences that the $MoSe_2$ crystals are grown on the SnS_2 with their hexagonal edges aligned. RHEED confirmed this even at fractional coverages. TEM-SAD also revealed that the edge alignment was nearly perfect (<1 deg of misalignment). In addition, LEED also showed a well ordered single crystal like surface. STM provided real space images of the grain morphologies of the $MoSe_2$ epilayer. In addition, the domains are separated by the antiphase domain boundaries, so named because these lead to phase differences between the scattered electrons from adjacent, otherwise identical domains. STM also revealed subtle structures resulting from the van der Waals interactions of the two lattices.

How does van der Waals epitaxy, as herein described, differ from conventional MBE? This is perhaps a most natural question as long as the deposition technique is concerned. In fact, there are no obvious differences in this regard from conventional MBE, such as GaAs growth. The essence of VDWE is, therefore, not the deposition process but instead refers to the resultant structure of films made up of 2D metal–chalcogen molecular units with strong bonding within the layers but separated by a van der Waals gap. As a result, the interface is smooth, abrupt and noninteractive. Lattice mismatch appears to manifest itself in more subtle ways as a result of the van der Waals interactions between the hard spheres but not via propagation of dislocations through the epilayer as a result of unsaturated bonding. In the present study, $SnS_2(0001)$ was used as the substrate, on which $MoSe_2$ was epitaxially grown. The lattice mismatch in this case is nearly 10%, however, it was demonstrated that $MoSe_2$ grows from the first layer with only subtle changes in its structure due to the two lattices going in and out of phase. The electronic structure of even this first layer was shown to be nearly identical to single crystalline $MoSe_2$.

While these features are unique to VDWE and not commonly observed in conventional MBE, many questions still remain about the mechanism of VDWE. One possibility is that the substrate electronic structure controls the orientation of the growing films.[12] The van der Waals interaction, mainly represented by a Lennard-Jones potential, may influence the epitaxy. The "wagon wheel" structures observed in STM images suggest strongly this possibility. Another possibility is based in classical nucleation and growth phenomena where the nucleation takes place at substrate defects and proceeds with no influence from the electronic structure of the substrate. In this case steps aligned with the crystallographic directions of the substrate (which can be directly imaged with the STM) nucleate the growth of the epilayer accounting for the rotational alignment. Recent work has demonstrated that VDWE is not restricted to the heteroepitaxial growth between layered materials[13] but can be extended to the growth on 3D materials, such as $CaF_2(111)$[14] and sulfur-terminated GaAs(111) surfaces.[15] These examples indicate that inertness of the surfaces as well as absence of surface dangling bonds appear to be prerequisites of the VDWE process. Future experiments will seek answers to the mechanism of VDWE and will also focus on the synthesis of more structurally and electronically complex structures with fewer defects while utilizing the flexibility of VDWE for selection of materials for substrates and epilayers.

V. CONCLUSIONS

The versatility of van der Waals epitaxy as a variation of on conventional MBE has been demonstrated by fabricating a $MoSe_2$ layer on a single crystalline SnS_2 substate, where the lattice mismatch is 10%. Combining *in situ* and *ex situ* techniques, a detailed characterization for the growth process and the heterointerface has been made. Although there is no covalent bonding between two layers, the van der Waals forces which hold the layers together in the pure crystal still operate on the epilayer. STM images of epilayers show unique structures resulting from the large lattice mismatch.

ACKNOWLEDGMENTS

Sue Riggs is acknowledged for technical assistance in the STM studies. We also acknowledgem the help of Mike VanKavelaar with the transmission electron microscopy. The present work is partially supported by Grant-in-Aid for Scientific Research from the Ministry of Education, Science and Culture of Japan.

[1] A. Koma, K. Sunouchi, and T. Miyajima, Microelectron. Eng. **2**, 129 (1984).
[2] A. Koma, K. Sunouchi, and T. Miyajima, J. Vac. Sci. Technol. B **3**, 724 (1985).
[3] G. A. Wiegers, A. Meetsma, R. J. Haange, and J. L. de Boer, Mater. Res. Bull. **23**, 1551 (1988).
[4] A. Koma, K. Sunouchi, and T. Miyajima, *Proceedings of the 17th International Conference on Physics in Semiconductors*, (Springer, New York, 1985), p. 1465.
[5] R. Spah, M. Lux-Steiner, M. Obergfell, and E. Bucher, Appl. Phys. Lett. **47**, 871 (1985).
[6] R. Spah, U. Elrod, M. Lux-Steiner, and E. Bucher, Appl. Phys. Lett. **43**, 9 (1983).
[7] V. Grasso, Ed., *Electronic Structure and Electronic Transitions in Layered Materials*, (Reidel, Dordrecht, 1986).
[8] (a) J. S. Stickney, S. R. Rosasco, T. Solomun, A. T. Hubbard, and B. A. Parinson, Surf. Sci. **136**, 15 (1984). (b) W. Jaegermann, F. S. Ohuchi, and B. A. Parkinson, *ibid.* **201**, 211 (1988).
[9] F. Hulliger, *Structural Chemistry of Layer-Type Phases*, edited by F. Levy, Vol. 5 in the Series Physics and Chemistry of Materials With Layered Structures (Reidel, Dordrecht, 1976).
[10] A. Koma and K. Yoshimura, Surf. Sci. **174**, 556 (1986).
[11] B. A. Parkinson, F. S. Ohuchi, K. Ueno, and A. Koma (in preparation).
[12] T. Miyazaki, M. Okazaki, and H. Aoki, Solid State Phys. (in Japanese) **24**, 37 (1989).
[13] K. Ueno, K. Saiki, T. Shimada, and A. Koma, J. Vac. Sci. Technol. A **8**, 68 (1990).
[14] A. Koma, K. Saiki, and Y. Sato, Appl. Surf. Sci. **41/42**, 451 (1989).
[15] K. Ueno, T. Shimada, K. Saiki, and A. Koma, Appl. Phys. Lett. **56**, 327 (1990).